

# Journal of Materials Chemistry C

Accepted Manuscript



This is an *Accepted Manuscript*, which has been through the Royal Society of Chemistry peer review process and has been accepted for publication.

*Accepted Manuscripts* are published online shortly after acceptance, before technical editing, formatting and proof reading. Using this free service, authors can make their results available to the community, in citable form, before we publish the edited article. We will replace this *Accepted Manuscript* with the edited and formatted *Advance Article* as soon as it is available.

You can find more information about *Accepted Manuscripts* in the [Information for Authors](#).

Please note that technical editing may introduce minor changes to the text and/or graphics, which may alter content. The journal's standard [Terms & Conditions](#) and the [Ethical guidelines](#) still apply. In no event shall the Royal Society of Chemistry be held responsible for any errors or omissions in this *Accepted Manuscript* or any consequences arising from the use of any information it contains.



Journal Name

ARTICLE

## Novel donor-acceptor carbazole and benzothiadiazole material for deep red and infrared emitting applications.

Przemyslaw Ledwon<sup>\*a</sup>, Pawel Zassowski<sup>a</sup>, Tomasz Jarosz<sup>a</sup>, Mieczyslaw Lapkowski<sup>a,b</sup>, Pawel Wagner<sup>c</sup>, Vladyslav Cherpak<sup>d</sup>, Pavlo Stakhira<sup>d</sup>

Received 00th January 20xx,  
Accepted 00th January 20xx

DOI: 10.1039/x0xx00000x

www.rsc.org/

A novel organic material (C1) with the structure D- $\pi$ -A- $\pi$ -D was synthesised and characterised. Carbazole was utilised as the electron donor and benzothiadiazole as the electron acceptor unit. Electrochemical, optical and electronic properties of the synthesised compound were studied. Compound C1 exhibits absorption in the visible and ultraviolet range with a high molar absorption coefficient. Strong solvatochromic effect was observed for its emission spectra. Electrochemical and spectroelectrochemical measurements were performed in order to estimate the properties of the molecule in different redox states. Electron Paramagnetic Resonance (EPR) measurement indicates delocalisation of radical cations and radical anions over different moieties. Interpretations of electrochemical and optical results are supported by DFT calculations. OLEDs based on C1 present efficient emission in red and infrared spectral ranges, with a quantum efficiency of 3.13% and current efficiency of 6.8 cd·A<sup>-1</sup>. The performance is considerably better than what has been reported for analogous devices, based on other carbazole and benzothiadiazole units.

### Introduction

Carbazole is an inexpensive material, which can be combined with a variety of conjugated units to yield new materials<sup>1</sup>. Carbazole derivatives are a promising class of organic molecules, finding application in optoelectronics, such as organic light emitting diodes (OLEDs)<sup>2–4</sup>, organic field effect transistors (OFETs)<sup>5,6</sup>, electrochromic devices<sup>7</sup>, dye sensitised solar cells (DSSCs)<sup>8</sup> and bulk heterojunction solar cells (BHJ)<sup>9,10</sup>. The most important features of carbazole-based materials are their high hole mobility<sup>6</sup>, high fluorescence quantum yields<sup>11</sup>, high molar extinction coefficients<sup>12</sup>, and the ability to undergo polymerisation<sup>13</sup>. Some properties, such as self-assembly behaviour<sup>14</sup>, aggregation-induced emission enhancement (AIEE)<sup>15</sup>, emission from excitons or exciplexes<sup>4,16,17</sup> and energy levels, can be modulated by altering the architecture of the molecule<sup>18</sup>.

Organic donor-acceptor (D-A) push-pull chromophores are an important group of  $\pi$ -conjugated materials with narrow band

gaps<sup>19–23</sup>. The choice of different, electron-rich and electron-poor units along the  $\pi$ -conjugated, organic backbone of the molecule affords control over the material functionality for organic electronic applications through the push-pull effect.<sup>24,25</sup> Moreover, the substitution pattern of carbazole modifies the molecule properties<sup>26,27</sup>.

The electron-accepting benzothiadiazole moiety is frequently used in the design of donor-acceptor (D-A) type of  $\pi$ -conjugated organic compounds<sup>28–32</sup>. This popularity stems from both the low position of its LUMO energy level and good stability of benzothiadiazole derivatives in the reduced state<sup>19</sup>. Moreover,  $\pi$ -conjugated organic materials, incorporating benzothiadiazole units in their backbone, present outstanding properties, suitable in different optoelectronic applications, such as broad light absorption in the visible range, low band gap, high electric conductivity, high optical contrast in different redox states and good charge separation.<sup>24,33–36</sup>

The concept of utilising benzothiadiazole as a moiety for photoemission applications is one found even in some older reports<sup>37</sup>. Recent years have brought about the development of new materials, containing benzothiadiazole units within their chemical structure. An array of compounds has been reported, both symmetrical, such as A- $\pi$ -D- $\pi$ -A, D- $\pi$ -A- $\pi$ -D and asymmetrical, such as A- $\pi$ -D, D<sub>1</sub>- $\pi$ -A- $\pi$ -D<sub>2</sub><sup>38,39</sup>. The choice of the donor, the acceptor and the linking moiety is what determines the properties of such a molecule. Through careful tailoring of this choice, the desired material properties can be obtained in a material.

<sup>a</sup> Silesian University of Technology, Faculty of Chemistry, 44-100 Gliwice, Strzody 9, Poland, ul. Marcina Strzody 9, 44-100 Gliwice, Poland.

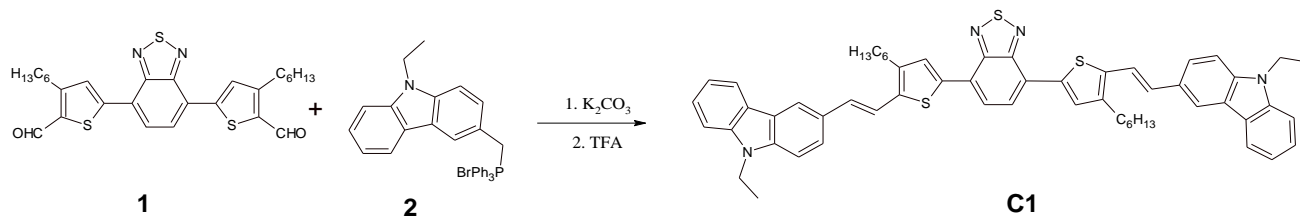
\*e-mail: przemyslaw.ledwon@polsl.pl; tel: +48 322371305

<sup>b</sup> Centre of Polymer and Carbon Materials, Polish Academy of Sciences, 41-819 Zabrze, Curie-Skłodowskiej 34, Poland

<sup>c</sup> ARC Centre of Excellence for Electromaterials Science and the Intelligent Polymer Research Institute, University of Wollongong, Australia

<sup>d</sup> Lviv Polytechnic National University, S. Bandera 12, 79013 Lviv, Ukraine

† Electronic Supplementary Information (ESI) available: simulated spin density of radical trication; OLED characteristics of devices with C1 layers with 80 and 160 nm. See DOI: 10.1039/x0xx00000x



Scheme 1 Synthesis of (C1)

Conjugated D-A materials find numerous applications as active layers for solar cells, organic light emitting diodes (OLEDs) and electrochromic devices. The use of D-A compounds in photovoltaics has become commonplace, however, their use in OLEDs remains limited, due to several difficulties. The most important property of push-pull systems, which limits their application in light emitting applications to only a part of the visible range, is the quenching of fluorescence with increasing dipole moment<sup>40</sup>. Generally, the stronger the push-pull effect in a system, the greater the red-shift of emission. For this reason strong push-pull organic  $\pi$ -conjugated molecules with efficient electroluminescence in the red and infrared range are rare. Infrared emitters are materials of particular interest, due to their possible applications in telecommunications, signalling and displays<sup>41</sup>. Among recent reports, pertaining to organic push-pull systems applied as red and IR emissive layers in OLEDs, are the works of Promarak et al<sup>42–44</sup>. These works report interesting properties for compounds based on a N-carbazyl moiety. The best results, however, have been reported for devices utilising push-pull systems that are complex and oligomeric in nature, which may prove to be a limiting factor for their application.

Here, we report our synthesis of the macromolecule C1, based on carbazole and benzothiadiazole, along with the results of its comprehensive investigation. Optical, redox and electronic properties were studied. C1 was used as an emissive layer in an OLED device, showing good performance.

## Results and discussion

### Synthesis

The C1 was obtained as a side product in the Wittig condensation of 1 and 2 in boiling benzene, with potassium carbonate as a base. We have employed solid – liquid phase transfer catalysis conditions, using 18-crown-6 as a catalyst. Because of relatively high reactivity of 2, we have found that those reaction settings gave the highest yield of the desired products. After condensation, C1 was obtained as a mixture of *E* and *Z* isomers. The isomer mixture was converted into pure, more thermodynamically stable, *E* isomer by treating it with trifluoroacetic acid at room temperature with almost quantitative yield.

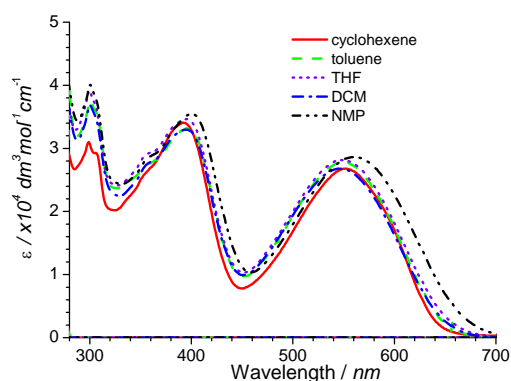
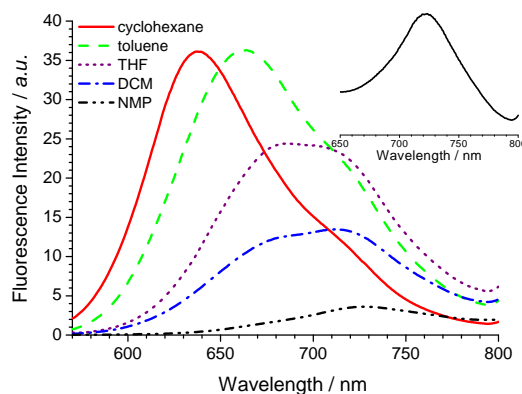
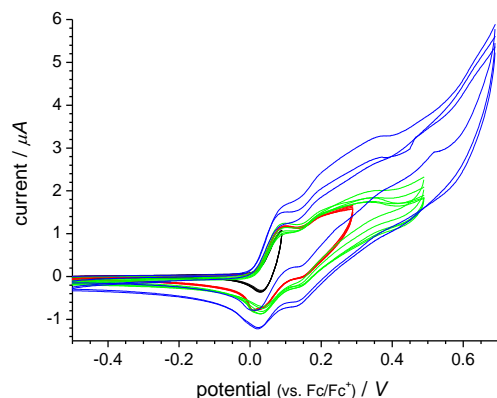


Fig. 1 UV-Vis-NIR spectra of C1 solutions in different solvents.

Fig. 2 Fluorescence spectra of  $2 \cdot 10^{-6}$  mol·dm<sup>-3</sup> C1 solutions in different solvents excited at 554 nm and solid state film (inset).

### Photophysical properties

The photophysical properties of compound C1 were measured by UV-Vis and fluorescence spectroscopy. The solvatochromic effect was determined by use of solvents with different polarity. UV-Vis spectra of C1 dissolved in different solvents show differences (Fig. 1). These indicate that the observed electronic transitions are affected by the medium.



**Fig. 3** Cyclic voltammetry of 1 mM (C1) solution during multiple oxidation; potential sweep rate  $0.1 \text{ V}\cdot\text{s}^{-1}$ ;  $0.1 \text{ M Bu}_4\text{NPF}_6/\text{DCM}$  electrolyte.

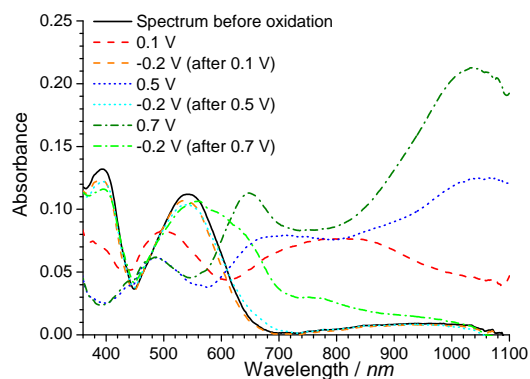


**Fig. 4** UV-Vis-NIR spectra of (C1) solution recorded at different potentials;  $0.1 \text{ M Bu}_4\text{NPF}_6/\text{DCM}$  electrolyte.

Strong charge transfer (CT) peaks dominate the visible range of **C1** solutions. This type of absorption bands occurs in some donor-acceptor organic molecules, for example other benzothiadiazole derivatives<sup>45</sup>. The high value of  $\epsilon$  (approximately  $2.7 \cdot 10^4 \text{ dm}^3\text{mol}^{-1}\text{cm}^{-1}$ ) of this peak is observed. Slightly more intensive  $\pi\text{-}\pi^*$  transition bands with  $\epsilon$  value of up to  $3.5 \cdot 10^4 \text{ M}^{-1}\text{cm}^{-1}$  are observed in the shorter wavelength range. Different solvatochromic effects were observed for both transition bands. The  $\lambda_{\text{max}}$  of  $\pi\text{-}\pi^*$  transitions shifts with increased solvent polarity from 391 nm (cyclohexane) to 400 nm (NMP). The  $\lambda_{\text{max}}$  of CT shifts from 544 nm (DCM) to 559 nm (NMP). This indicates that some additional factors influence the charge transfer absorption bands, such as polarizability and intermolecular interactions<sup>46</sup>.

A strong solvatochromic fluorescence effect is observed (Fig. 2). Different sub-bands of fluorescence spectra are observed. The rebuild and shift of the emission is observed with changed solvents. The intensity of the two dominant sub-bands depends strongly on the polarity of solvents. Excitation by 554 nm gives fluorescence spectra with an emission

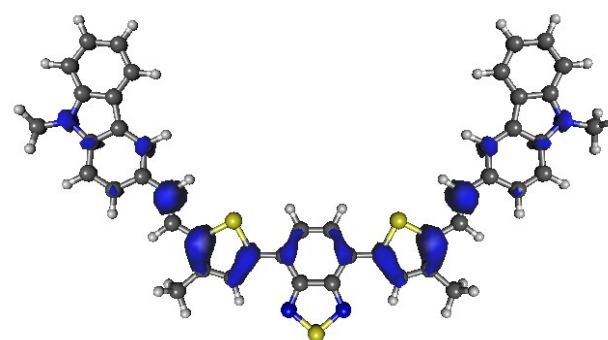
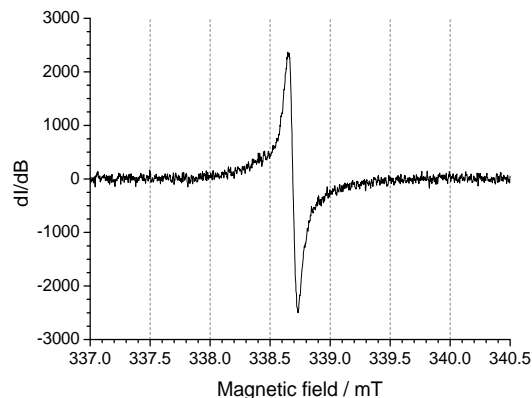


**Fig. 5** EPR spectra of radical cations obtained with constant electrolysis: C1 ( $E=0.1\text{V}$  vs.  $\text{Fc}/\text{Fc}^+$ ) (top) Measurement conditions: modulation amplitude:  $0.02\text{mT}$ , microwave power:  $2\text{mW}$ . A simulated spin density (isovalue= $0.002$ ) is presented, calculated with DFT/ $\text{uB3LYP}/6\text{-}31\text{G(d)}$  method (bottom).

maximum ( $\lambda_{\text{em}}$ ) at 637 nm in cyclohexane and 661 nm in toluene. In the case of more polar solvents, the  $\lambda_{\text{em}}$  shifts up to 683 nm in THF, 712 nm in DCM and 724 nm in NMP. Such effects usually have complex character<sup>47</sup>. In our case, two different phenomena occur: bathochromic shift with increased solvents polarity and different ratio of two sub-bands.

The large solvatochromic fluorescence effect was earlier observed in similar systems, with strong ambipolar character<sup>48,49</sup>. The modification of energy levels of excited states with increased polarity of solvents explains the bathochromic fluorescence effect of **C1** solutions. The emissive intramolecular charge transfer state is more strongly solvated with increased environment polarity. The charge separation is enhanced and the energy is lowered, resulting in the bathochromic shift of emission.

The possible explanation of occurrence of two sub-bands with different intensity ratios is the formation of J-Aggregates.<sup>50</sup> The increased solvent polarity can induce formation of aggregates. The formation of J-Aggregates results in the

emission in the lower energy range compared to non-aggregated molecules.

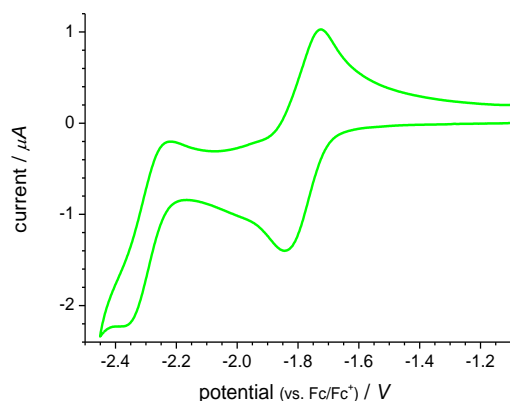


**Fig. 6** Cyclic voltammetry of 1 mM C1 solution during reduction; potential sweep rate  $0.1 \text{ V}\cdot\text{s}^{-1}$ ;  $0.1 \text{ M}$

**Table 1** Electronic properties estimated from electrochemical, optical measurement and DFT calculations

IP	$E_{\text{HOMOel}}$	$E_{\text{HOMOcalc}}$	EA	$E_{\text{LUMOel}}$	$E_{\text{LUMOcalc}}$	$E_{\text{gel}}$	$E_{\text{gopt}}$	$E_{\text{gcalc}}$
[eV]	[eV]	[eV]	[eV]	[eV]	[eV]	[eV]	[eV]	[eV]
5.1	-5.1	-4.68	3.4	-3.4	-2.70	1.7	1.89	1.98

### Redox properties

Cyclic voltammetry was used to characterise redox and electronic properties of studied compounds. UV-Vis-NIR and EPR spectroelectrochemical measurements, supported by DFT calculations were used to elucidate redox reactions.

CV curves of both compounds in the anodic range present multistep oxidation (Fig. 3). The redox pairs of **C1** are located at 0.06 V and 0.30 V. After exceeding this potential range the CV curve takes a complex shape with overlapping peaks. Multiple CV scanning in the exceeded potential range up to 0.68 V led to the formation of a greenish film at the electrode surface. Moreover, in the subsequent two cycles a current increase is observed. Further scanning, however, does not see this behaviour continued. This can be explained by electrode surface becoming covered by a poorly conductive polymer film<sup>51</sup>.

The UV-Vis spectra of thin solution layers were recorded during oxidation, according to a procedure published earlier<sup>52</sup>. At the beginning of oxidation, at potential 0.1 V the decrease of neutral molecule transition bands (Fig. 4) and simultaneous appearance of new broad transition bands, located at approximately 798 nm and 495 nm, is observed. EPR signals were recorded in the same conditions (Fig. 5). A single EPR line was observed. The product of oxidation is paramagnetic, i.e. it has an unpaired electron in its structure. A single line instead of multiline spectra indicates the delocalisation of the observed radical cation. Spin density, simulated by DFT calculations confirms the delocalisation of the radical, showing

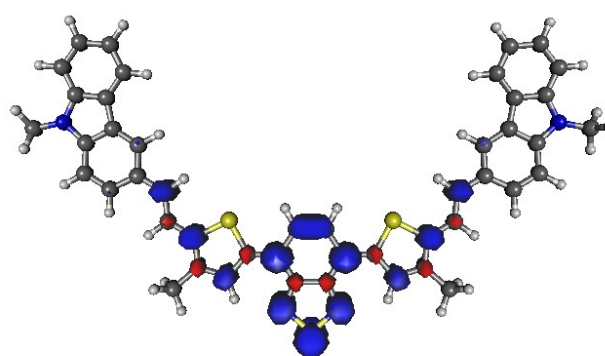
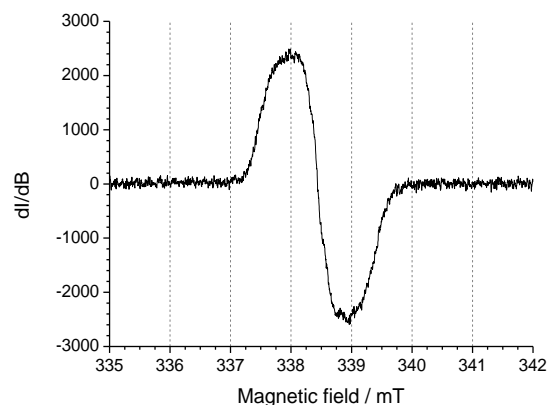


**Fig. 7** EPR spectra of radical anion obtained with constant electrolysis ( $E = -1.7 \text{ V vs. Fc/Fc}^+$ ) of **C1** (top). Measurement conditions: modulation amplitude:  $0.05 \text{ mT}$ , microwave power:  $2 \text{ mW}$ . A simulated spin density (isovalue =  $0.002$ ) is presented, calculated with DFT/ub3LYP/6-31G(d) method

the highest spin density at diamagnetic atoms in the centre of the molecule. The change of potential to  $-0.2 \text{ V}$  results in reduction of the radical cations to neutral **C1** molecules. This indicates the reversibility of the oxidation in this potential range.

At higher oxidation potentials at  $0.5 \text{ V}$  and  $0.7 \text{ V}$ , corresponding to subsequent oxidation steps, new absorption bands start to dominate. The UV-Vis spectrum recorded after oxidation and subsequent reduction at  $-0.2 \text{ V}$  of a compound **C1** solution shows new absorption bands of neutral molecules at longer wavelengths. This indicates formation of products with a longer conjugated bond system. This behaviour is in accordance with spectroelectrochemical results of other carbazole-based compounds, the detailed analysis of which shows the formation of linkage between carbazole units<sup>5,13,53</sup>. Both cyclic voltammetry and spectroelectrochemical measurements indicate poor electrochemical properties of the polymer film deposited on the electrode. It is related to high reactivity of vinyl linkers in these conditions, leading to side reactions. Based on this data we found that the exact mechanism of formation of conjugated polymer is a

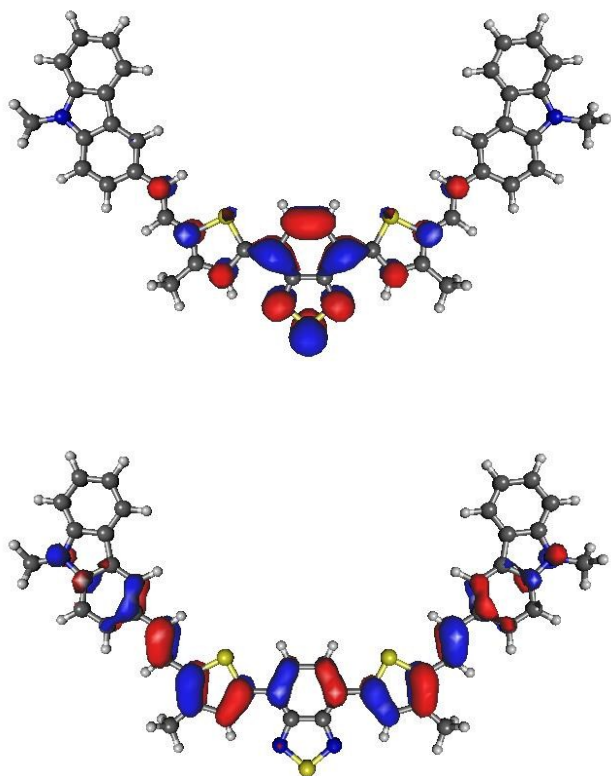


**Fig. 8** Calculated shapes of LUMO (top) and HOMO (bottom) orbitals of (**C1**), obtained with DFT/B3LYP/6-31(d). Isovalue in each case is equal to 0.03.

modification of already known mechanism of N-alkylcarbazole electropolymerisation, which proceeds through the 3 and 6 positions of carbazole moiety.<sup>54,55</sup> As the first step of oxidation step creates a stable radical, molecules having higher oxidation levels must be responsible for polymerisation. Knowing that this kind of process is usually associated with coupling of radicals, we concluded that radical trications of **C1** may couple with each other forming a polymer on the surface of the electrode.

In order to validate this assumption, we have calculated the spin density of such molecule state (Fig. S1). In contrast to radical cation, this state of molecule presents a spin density at edges of the structure, allowing for polymerisation of the compound.

CV curves of **C1** recorded in the cathodic range show two redox pairs (Fig. 6). The first reversible pair is located at -1.78 V and the second, quasi-reversible pair at -2.3 V. The electrochemical reversible reduction results mainly from the presence of benzothiadiazole unit in the molecule structure. This electron acceptor unit consists of two electron-withdrawing imine (C=N) nitrogen atoms, which stabilise radical anions<sup>56</sup>. EPR spectra of the radical anion of **C1** are shown in Fig. 7. At the potential of the first reduction peak only a single broad line is observed. Contrary to other examples of benzothiadiazole-based radical anions, no

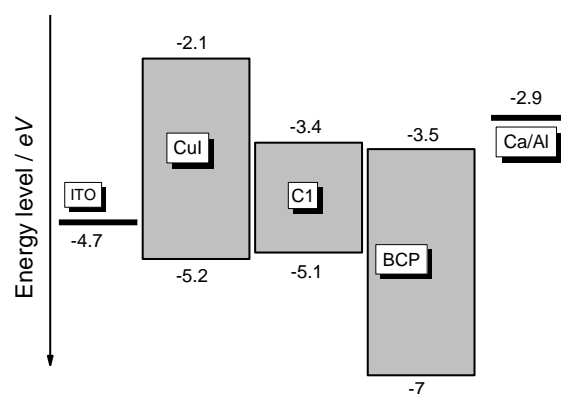


**Fig. 9** Energy diagram of OLED devices

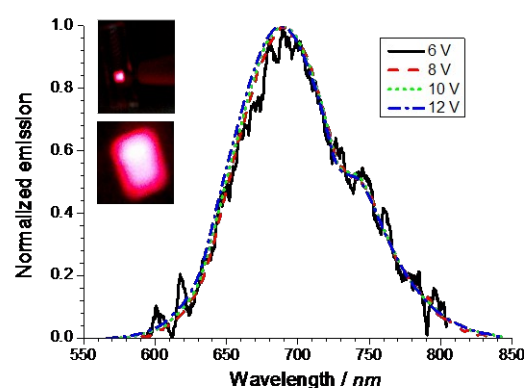


**Fig. 10** Normalized electroluminescence spectra of device with ITO/CuI/C1/BCP/Ca/Al architecture recorded at different potentials.

hyperfine coupling splitting of the EPR line can be observed. This indicates wider delocalisation of the radical anion, rather than only at the benzothiadiazole unit<sup>57</sup>. At the same time, the broad character of the EPR line suggests that interaction of spin with further paramagnetic nuclei (such as hydrogen atoms of vinyl linker), results in a broad single line shape of EPR line. Simulated spin density of radical anion confirms these observations.

#### Electronic properties

The theoretical values of HOMO ( $E_{\text{HOMOcalc}}$ ) and LUMO ( $E_{\text{LUMOcalc}}$ ) energy levels were calculated by DFT. The shape of HOMO and LUMO orbitals is presented in Fig. 8. The HOMO spreads over the entire backbone. HOMO overlaps with radical cation spin density. It provides important information about the oxidation mechanism. Higher oxidation states are required to formation for carbazole coupling. Electron removal from deeper lying orbitals (e.g. HOMO-1) could result in formation of radicals localised at the carbazole moieties.

In the case of LUMO level strong localisation at benzothiadiazole unit occurs. Furthermore, strong localisation of LUMO level leads to partial separation of frontier orbital position in **C1**. This effect is probably responsible for strong

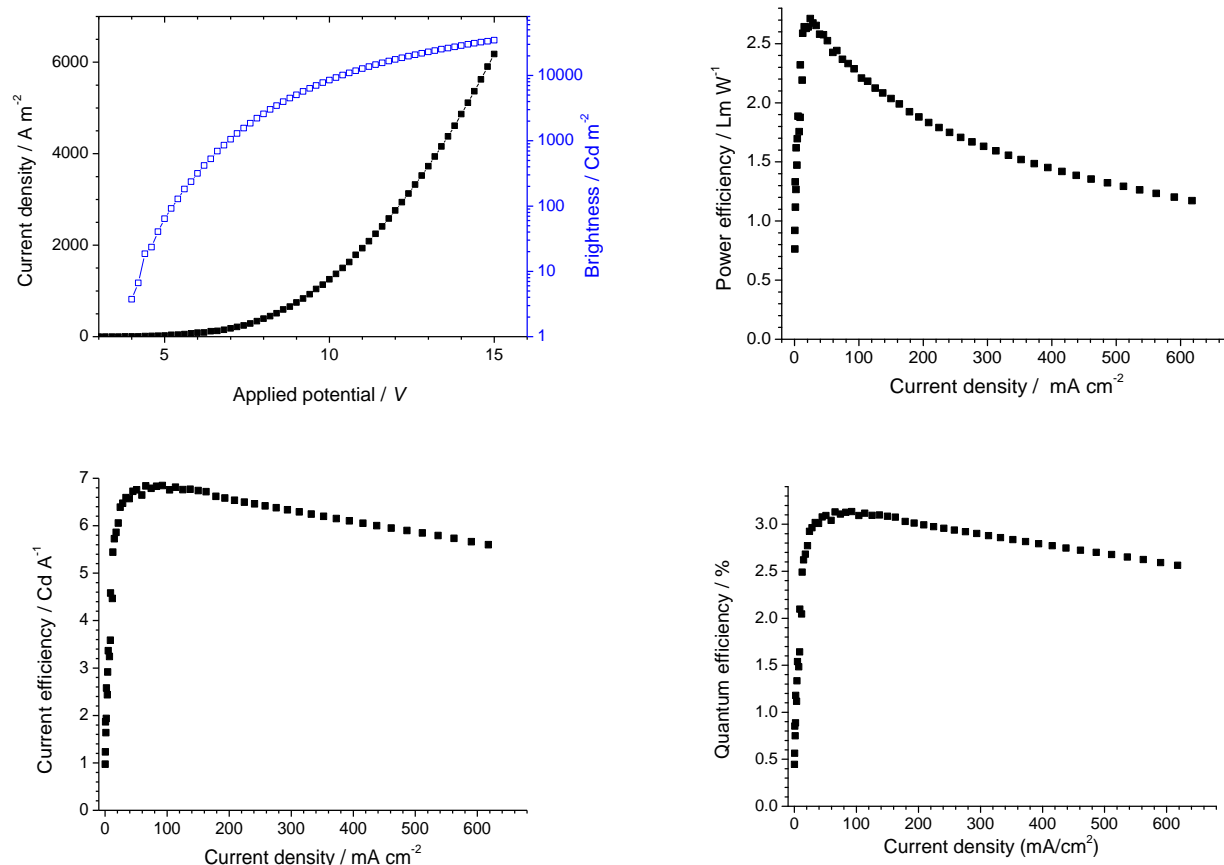


Fig. 11 Operating parameters of a prototype OLED based on 120nm layer of C1 (ITO/CuI/C1/BCP/Ca/Al).

**Table 2** Characterization of devices with ITO/CuI/C1/BCP/Ca/Al architecture with different thickness of C1 layer

C1-layer thickness [nm]	$V_{on}$ [V]	$CE_{max}$ [ $cd \cdot A^{-1}$ ] (V [V])	$PE_{max}$ [ $lm \cdot W^{-1}$ ]	Brightness [ $cd \cdot m^{-2}$ ]	$EQE_{max}$ [%]
80	3.3	0.48 (11)	0.22	4060	0.22
120	4	6.8 (9.5)	2.7	34800	3.13
160	3.6	2.5 (5.8)	1.5	7340	1.12

differences in solvatochromic properties discussed in previous spectral measurement section.

Ionisation potential (IP) and electron affinity (EA) were estimated from oxidation onset potential ( $E_{ox\ onset}$ ) and reduction onset potential ( $E_{red\ onset}$ ) respectively (Table 1). In order to compare with other reports,  $E_{HOMOel}$  and  $E_{LUMOel}$  estimated from CV measurement are presented. At this point, it should be mentioned that these values should be considered with a degree of caution, because CV curves can give only approximate  $E_{HOMOel}$  and  $E_{LUMOel}$  values, affected by the measurement conditions.

#### OLED characterisation

In order to check the practical application of C1 compound, the OLED devices with structure ITO/CuI/C1/BCP/Ca/Al were

fabricated (Fig.9). A number of OLEDs, utilising compound C1 as the emissive layer, has been manufactured, with the structural parameters of the devices being varied. The most beneficial operating parameters have been registered for the device with 120 nm layer of C1. The thickness of the electroactive layer, departing from that of the top-performing device, has turned out to afford the most tolerance in terms of decaying operational parameters of the device, with alterations in other variables leading to a dramatic loss of efficiency. The best device performance was obtained at 120 nm C1 thickness, which can be explained by superposition of two main factors: the best balance of charge carriers and the best light extraction<sup>58</sup>.

Electroluminescence of the device is in the deep red and partially in the infrared range, with a maximum electroluminescence intensity observed at 688 nm. The electroluminescence spectra of the device change intensity at different voltage bias. Normalised electroluminescence spectra of the device, with a 120 nm layer of C1 are shown at Fig. 10. The normalised spectra recorded in the range from 6 V to 12 V are the same, indicating good stability of device. The current density-voltage (I-V) and brightness-voltage curves are presented in Fig. 11. The turn on voltage ( $V_{on}$ ) of device is as low as 4 V. The brightness of the device reaches 1000  $cd \cdot m^{-2}$  at 7 V, 10000  $cd \cdot m^{-2}$  at 10.4 V and 34800  $cd \cdot m^{-2}$  at 15 V.

The device exhibits the maximum current efficiency value ( $CE_{max}$ ) of  $6.8 \text{ cd}\cdot\text{A}^{-1}$  on voltage (V) 9.5 V, maximum power efficiency ( $PE_{max}$ ) of  $2.7 \text{ Lm}\cdot\text{W}^{-1}$  and maximum quantum efficiency ( $EQE_{max}$ ) as high as 3.13 %. These results are better than OLEDs based on other similar ambipolar carbazole-benzothiadiazole structures<sup>59,60</sup>.

## Experimental

### Synthetic procedures

4,7-bis(5-formyl-3-hexylthien-2-yl)benzo-2,1,3-thiadiazole (**1**)<sup>61</sup>, triphenylmethyl(9-ethylcarbazol-3-yl) phosphonium bromide (**2**)<sup>62</sup> were synthesised according to previously published procedures. All other chemicals were available commercially and were used without additional purification, unless stated differently. NMR spectra were recorded on a Bruker Avance 400 spectrometer. The following abbreviations were used: s = singlet, d = doublet, dd = doublets of doublets, ddd = doublets of doublets of doublets, t = triplet, m = multiplet. All coupling constants J were measured in hertz (Hz). Chemical shifts are reported in parts-per-million (ppm). Tetramethylsilane was used as the internal reference. Mass spectra were recorded on Polaris Q or Hewlett Packard 5973. The synthetic procedures were not optimised.

(E, E) 4,7-Bis(5-(2-(9-ethylcarbazol-3-yl)ethenyl)-4-hexylthien-2-yl)benzo-2,1,3-thiadiazole (**C1**): 4,7-bis(5-formyl-4-hexylthien-2-yl)benzo-2,1,3-thiadiazole (**1**) (1.60 g, 3.1 mmol), (9-ethylcarbazol-3-yl)methyltriphenylphosphonium bromide (**2**) (1.68 g, 3.1 mmol) and catalytic amount of 18-crown-6 were dissolved in dry benzene (100 mL) then anhydrous potassium carbonate (4.28 g, 31 mmol) was added (Scheme 1). The resulting slurry was refluxed for 1 hour then cooled down, filtered and the solvent was removed under reduced pressure at 50°C. The remaining raw product was purified on silica, using mixture of dichloromethane (DCM) and hexane (7:3) as an eluent. The compound was collected in the first major fraction. After solvent evaporation, the resulting solid was dissolved in DCM (9 mL), to which trifluoroacetic acid (9 mL) was added, followed by water (3 mL). The resulting dark mixture was stirred vigorously for 30 minutes, after which the organic layer was separated, washed with water and diluted ammonia, dried over magnesium sulphate and filtered through a pad of silica, using DCM as an eluent. After solvent evaporation, the solid was dissolved in a minimal amount of DCM and precipitated with methanol to give the product as a dark powder.

<sup>1</sup>H NMR (400 MHz, 318 K, CDCl<sub>3</sub>)  $\delta$ : 8.21 (dd, 2H, J = 1.6 and 0.6 Hz, Carb-H4), 8.14 (ddd, 2H, J = 7.8, 1.2 and 0.8 Hz, Carb-H5), 7.98 (s, 2H, Ar-H), 7.82 (s, 2H, Th-H), 7.67 (dd, 2H, J = 8.7 and 1.6 Hz, Carb-H2), 7.48 (ddd, 2H, J = 8.3, 7.8 and 1.0 Hz, Carb-H6), 7.42 – 7.36 (m, 4H, Carb-H1, H8), 7.33 (d, 2H, J = 16.0 Hz, vinyl-H), 7.25 (ddd, 2H, J = 8.3, 7.8 and 1.2 Hz, Carb-H7), 7.23 (d, 2H, J = 16.0 Hz, vinyl-H), 4.36 (q, 4H, J = 7.3 Hz, N-CH<sub>2</sub>), 2.81 (t, 4H, J = 7.9 Hz, Th-CH<sub>2</sub>), 1.80 – 1.71 (m, 4H, Th-CH<sub>2</sub>-CH<sub>2</sub>-Alk), 1.51 – 1.46 (m, 4H, Th-CH<sub>2</sub>-CH<sub>2</sub>-CH<sub>2</sub>-Alk), 1.45 (t, 6H, J = 7.3 Hz, N-CH<sub>2</sub>-CH<sub>3</sub>), 1.41 – 1.33 (m, 8H, Th-Alk-CH<sub>2</sub>-CH<sub>2</sub>-CH<sub>3</sub>), 0.93 (t,

6H, J = 7.1 Hz, Th-Alk-CH<sub>3</sub>); <sup>13</sup>C NMR (100 MHz, CDCl<sub>3</sub>)  $\delta$ : 152.7, 145.5, 140.4, 138.9, 135.7, 130.5, 129.8, 128.6, 125.9, 125.5, 125.2, 124.4, 123.4, 123.0, 122.3, 120.6, 119.1, 118.7, 117.5, 108.7, 108.6, 37.7, 31.8, 31.0, 29.2, 28.7, 22.7, 14.1, 13.9; HRMS (ESI, (M+)<sup>+</sup>): found: 907.3867, requires for C<sub>58</sub>H<sub>59</sub>N<sub>4</sub>S<sub>3</sub>: 907.3896.

### Electrochemical measurement

Cyclic voltammetry experiments were performed on CH Instrument Electrochemical Analyzer model 620. Measurement was carried out in CH<sub>2</sub>Cl<sub>2</sub> (DCM) (Sigma Aldrich  $\geq 99.8\%$ ) or tetrahydrofuran (THF) (Acros Organics, 99.5%, Extra dry) containing 0.1M tetrabutylammonium hexafluorophosphate (Bu<sub>4</sub>NPF<sub>6</sub>) (Sigma Aldrich 98%) as a supporting electrolyte. Pt wire served as working electrode, Pt spiral as a counter electrode. An Ag pseudo-reference electrode was used and its exact potential was calibrated versus ferrocene/ferrocenium redox couple. All solutions were purged with argon before measurement.

The oxidation potential ( $E_{ox}$ ) and oxidation onset potential ( $E_{ox \text{ onset}}$ ) were determined from measurement in CH<sub>2</sub>Cl<sub>2</sub> solution. The reduction potential ( $E_{red}$ ) and oxidation onset potential ( $E_{red \text{ onset}}$ ) were determined from measurement in THF solution. Different solvents were chosen due to different potential window in the cathodic and anodic range with CH<sub>2</sub>Cl<sub>2</sub> suitable for oxidation and THF for reduction.

### Spectral measurement

UV-Vis measurements were carried out on 8453 Hewlett Packard spectrophotometer, while fluorescence measurements were performed on F-2500 Hitachi fluorescence spectrometer. Measurements were carried out in cyclohexane (Sigma Aldrich, 99% for spectroscopy), toluene (POCH, 99.8%), THF (Acros Organics, 99.5%, Extra dry), dichloromethane (Sigma Aldrich  $\geq 99.8\%$ ) and N-Methyl-2-pyrrolidone (NMP) (Fluorochem, 99.8%). UV-Vis spectra were recorded for solution in 2 mm cuvette.

### DFT calculations

DFT calculations were performed using the B3LYP<sup>63–65</sup> hybrid functional with 6-31G(d) basis set. Ground state geometry was optimised, without symmetry constraints, to a local minimum, which was followed by frequency calculations. In order to speed up the calculations, alkyl chains were simplified down to methyl groups. No imaginary frequencies were detected, proving that the obtained geometry was a local minimum. All calculations were carried out with the polarisable continuum model<sup>66</sup>, using DCM as a solvent in order to simulate the solution effects. Properties of radical cations and radical anions were simulated by setting the charge of the molecule to +1 and -1 respectively, while the multiplicity was set to 2. All calculations were carried out with Gaussian 09 software<sup>67</sup>. Input files and plots were prepared with Gabedit software<sup>68</sup>.

### EPR spectroelectrochemical experiments

EPR measurements were carried out in 1mM solutions of an investigated compound in 0.1 M Bu<sub>4</sub>NPF<sub>6</sub>/DCM electrolyte. A custom-made cylindrical quartz cell was used, equipped with a platinum wire working electrode, an auxiliary electrode in the

form of a platinum spiral and silver wire as a pseudo-reference electrode. The experiments were performed using a JEOL JES-FA 200, X-band CW-EPR spectrometer operating at 100 kHz field modulation.

#### Device fabrication

The electroluminescent devices were fabricated by means of vacuum deposition of organic semiconductor layers and metal electrodes onto pre-cleaned ITO-coated glass substrate at a vacuum of  $10^{-5}$  Torr. The device was fabricated through the step-by-step deposition of various functional layers. BCP and CuI was used for the hole- and electron-transporting layers, respectively<sup>69</sup>. The Ca layer topped with an aluminium (Al) layer was used as the cathode. The structure of the fabricated device was as follows: ITO/CuI/C1/BCP/Ca/Al. The active area of the obtained device was a 3mm x 6mm rectangle.

Characteristics of the current density-voltage and luminance-voltage dependences were measured with a semiconductor parameter analyser (HP 4145A). Devices were tested immediately after fabrication to avoid passivation in contact with air. The measurement of brightness was performed using a calibrated photodiode. The photodiode was placed in front of an OLED device, in a dark room, using the methods described in Ref. <sup>70</sup>. The EQE values were determined by using the equations presented in Ref. <sup>71</sup>. The electroluminescence spectra of the prototype OLED devices were recorded with an Ocean Optics USB2000 spectrometer.

#### Conclusions

Synthesis and characterisation of the new material with D- $\pi$ -A- $\pi$ -D is presented. Molecule **C1** undergoes multiple oxidation steps. The first oxidation and reduction steps the most important from the point of view of application in different optoelectronic and photovoltaic applications are reversible. Subsequent oxidation and reduction steps lead to multiple reactions such as vinyl side-reactions and carbazole coupling. The EPR study, supported by DFT calculations reveals the delocalisation of radical anion mainly at benzothiadiazole moiety. The radical cation is delocalised over nearly the entirety of the molecule. The application in OLED devices of compound C1 was checked. Good efficiency, with a quantum efficiency as high as 3.13 % indicates that C1 compound is a promising candidate for red and infrared applications. Electroluminescence is not strongly affected by quenching in the solid state, which is commonly observed for other D-A compounds. This conclusion can be especially valuable, when considering low molecular weight materials with shifted electroluminescence to the NIR range. The modification of the C1 structure in the direction of enhanced conjugation length and lower energy gap can result in a material with full emission in the NIR range.

#### Acknowledgements

The financial support of the Marie Curie International Research Staff Exchange Scheme within FP7-Peoples EU project no

PIRSES-GA-2013-612670 is gratefully acknowledged. Research presented in this work has been partially carried out at the Laboratory of Advanced Spectroelectrochemical Studies, established with financial contribution of the Polish National Science Centre grant no. 2011/03/D/ST5/06042. Pawel Wagner acknowledges ARC Centre of Excellence for Electromaterials Science, Centre for Cooperative Research (CRC) and ARC Discovery Grant Scheme. This research was supported in part by PL-Grid Infrastructure.

#### Notes and references

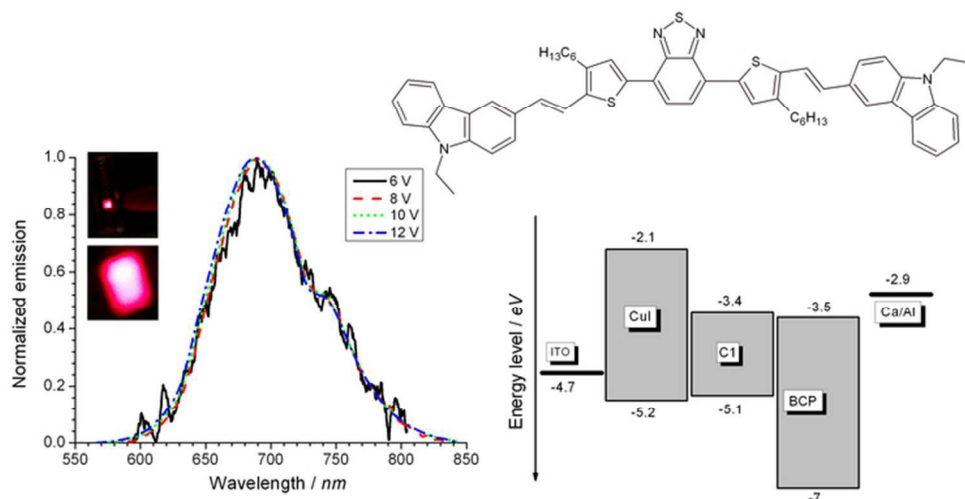
- 1 J. V. Grazulevicius, P. Strohriegel, J. Pieliowski and K. Pieliowski, *Prog. Polym. Sci.*, 2003, **28**, 1297–1353.
- 2 W. Jiang, Z. Ge, P. Cai, B. Huang, Y. Dai, Y. Sun, J. Qiao, L. Wang, L. Duan and Y. Qiu, *J. Mater. Chem.*, 2012, **22**, 12016–12022.
- 3 C. W. Lee, Y. Im, J.-A. Seo and J. Y. Lee, *Chem. Commun. (Camb.)*, 2013, **49**, 9860–2.
- 4 H. Uoyama, K. Goushi, K. Shizu, H. Nomura and C. Adachi, *Nature*, 2012, **492**, 234–238.
- 5 R. R. Reghu, J. V. Grazulevicius, J. Simokaitiene, A. Miasojedovas, K. Kazlauskas, S. Jursenas, P. Data, K. Karon, M. Lapkowski, V. Gaidelis and V. Jankauskas, *J. Phys. Chem. C*, 2012, **116**, 15878–15887.
- 6 G.-P. Chang, C.-N. Chuang, J.-Y. Lee, Y.-S. Chang, M. Leung and K.-H. Hsieh, *Polymer (Guildf.)*, 2013, **54**, 3548–3555.
- 7 A. Aydin and İ. Kaya, *J. Electroanal. Chem.*, 2013, **691**, 1–12.
- 8 J. Tang, J. Hua, W. Wu, J. Li, Z. Jin, Y. Long and H. Tian, *Energy Environ. Sci.*, 2010, **3**, 1736–1745.
- 9 J. Li and A. Grimsdale, *Chem. Soc. Rev.*, 2010.
- 10 J. Lee, S. B. Jo, M. Kim, H. G. Kim, J. Shin, H. Kim and K. Cho, *Adv. Mater.*, 2014, **26**, 6706–6714.
- 11 W.-Y. Lai, D. Liu and W. Huang, *Macromol. Chem. Phys.*, 2011, **212**, 445–454.
- 12 S. Cai, G. Tian, X. Li, J. Su and H. Tian, *J. Mater. Chem. A*, 2013, **1**, 11295–11305.
- 13 R. R. Reghu, J. V. Grazulevicius, J. Simokaitiene, T. Matulaitis, A. Miasojedovas, K. Kazlauskas, S. Jursenas, P. Data, M. Lapkowski and P. Zassowski, *Dye. Pigment.*, 2013, **97**, 412–422.
- 14 Z. Ding, R. Xing, X. Wang, J. Ding, L. Wang and Y. Han, *Soft Matter*, 2013, **9**, 10404–10412.
- 15 W. Huang, F. Tang, B. Li, J. Su and H. Tian, *J. Mater. Chem. C*, 2014, **2**, 1141–1148.
- 16 K. Brunner, A. van Dijken, H. Börner, J. J. a M. Bastiaansen, N. M. M. Kiggen and B. M. W. Langeveld, *J. Am. Chem. Soc.*, 2004, **126**, 6035–6042.
- 17 A. Michaleviciute, E. Gurskyte, D. Y. Volyniuk, V. V. Cherpak, G. Sini, P. Y. Stakhira and J. V. Grazulevicius, *J. Phys. Chem. C*, 2012, **116**, 20769–20778.
- 18 N. Blouin, A. Michaud, D. Gendron, S. Wakim, E. Blair, R. Neagu-Plesu, M. Belletête, G. Durocher, Y. Tao and M.

- Leclerc, *J. Am. Chem. Soc.*, 2008, **130**, 732–742.
- 19 K. Takimiya, I. Osaka and M. Nakano, *Chem. Mater.*, 2014, **26**, 587–593.
- 20 P. Ledwon, A. Brzeczek, S. Pluczyk, T. Jarosz, W. Kuznik, K. Walczak and M. Lapkowski, *Electrochim. Acta*, 2014, **128**, 420–429.
- 21 Z. Zhang and J. Wang, *J. Mater. Chem.*, 2012, **22**, 4178–4187.
- 22 E. Kozma and M. Catellani, *Dye. Pigment.*, 2013, **98**, 160–179.
- 23 S. S. Krompiec, M. M. Filapek, I. Grudzka, S. Kula, A. Słodek, Ł. Skórka, W. Danikiewicz, P. Ledwon, M. Lapkowski and P. Łukasz Skórka, *Synth. Met.*, 2013, **165**, 7–16.
- 24 M. Scarongella, A. Laktionov, U. Rothlisberger and N. Banerji, *J. Mater. Chem. C*, 2013, **1**, 2308–2319.
- 25 J. Kim, Y. S. Kwon, W. S. Shin, S.-J. Moon and T. Park, *Macromolecules*, 2011, **44**, 1909–1919.
- 26 S. Kato, S. Shimizu, A. Kobayashi, T. Yoshihara, S. Tobita and Y. Nakamura, *J. Org. Chem.*, 2014, **79**, 618–29.
- 27 S. Kato, H. Noguchi, A. Kobayashi, T. Yoshihara, S. Tobita and Y. Nakamura, *J. Org. Chem.*, 2012, **77**, 9120–9133.
- 28 B. Fu, J. Baltazar, A. R. Sankar, P.-H. Chu, S. Zhang, D. M. Collard and E. Reichmanis, *Adv. Funct. Mater.*, 2014, **24**, 3734–3744.
- 29 Y. Jiang, D. Yu, L. Lu, C. Zhan, D. Wu, W. You, Z. Xie and S. Xiao, *J. Mater. Chem. A*, 2013, **1**, 8270–8279.
- 30 M. Sendur, A. Balan, D. Baran, B. Karabay and L. Toppare, *Org. Electron.*, 2010, **11**, 1877–1885.
- 31 H. Shang, H. Fan, Y. Liu, W. Hu, Y. Li and X. Zhan, *Adv. Mater.*, 2011, **23**, 1554–1557.
- 32 A. Durmus, G. E. Gunbas, P. Camurlu and L. Toppare, *Chem. Commun. (Camb)*, 2007, 3246–3248.
- 33 M. L. Keshtov, D. V. Marochkin, V. S. Kochurov, A. R. Khokhlov, E. N. Koukaras and G. D. Sharma, *J. Mater. Chem. A*, 2014, **2**, 155–171.
- 34 S. Pelz, J. Zhang, I. Kanelidis, D. Klink, L. Hyzak, V. Wulf, O. J. Schmitz, J.-C. Gasse, R. Frahm, A. Pütz, A. Colsmann, U. Lemmer and E. Holder, *European J. Org. Chem.*, 2013, **2013**, 4761–4769.
- 35 J. Roncali, *Chem. Rev.*, 1992, **92**, 711–738.
- 36 P. J. Skabara, R. Berridge, I. M. Serebryakov, A. L. Kanibolotsky, L. Kanibolotskaya, S. Gordeyev, I. F. Perepichka, N. S. Sariciftci and C. Winder, *J. Mater. Chem.*, 2007, **17**, 1055–1062.
- 37 F. S. Mancilha, B. A. DaSilveira Neto, A. S. Lopes, P. F. Moreira, F. H. Quina, R. S. Gonçalves and J. Dupont, *European J. Org. Chem.*, 2006, 4924–4933.
- 38 R. Misra and P. Gautam, *Org. Biomol. Chem.*, 2014, **12**, 5448–5457.
- 39 P. Gautam, R. Maragani and R. Misra, *RSC Adv.*, 2015, **5**, 18288–18294.
- 40 G. Ulrich, A. Barsella, A. Boeglin, S. Niu and R. Ziessel, *ChemPhysChem*, 2014, **15**, 2693–2700.
- 41 G. Qian and Z. Y. Wang, *Chem. – An Asian J.*, 2010, **5**, 1006–1029.
- 42 A. Thangthong, N. Prachumrak, T. Sudyoadsuk, S. Namuangruk, T. Keawin, S. Jungstittiwong, N. Kungwan and V. Promarak, *Org. Electron. physics, Mater. Appl.*, 2015, **21**, 117–125.
- 43 T. Khanasa, N. Prachumrak, R. Rattanawan, S. Jungstittiwong, T. Keawin, T. Sudyoadsuk, T. Tuntulani and V. Promarak, *Chem. Commun. (Camb)*, 2013, **49**, 3401–3.
- 44 T. Sudyoadsuk, P. Moonsin, N. Prachumrak, S. Namuangruk, S. Jungstittiwong, T. Keawin and V. Promarak, *Polym. Chem.*, 2014, **5**, 3982–3993.
- 45 P. Ledwon, N. Thomson, E. Angioni, N. J. Findlay, P. J. Skabara and W. Domagala, *RSC Adv.*, 2015, **5**, 77303–77315.
- 46 R. Nandy and S. Sankararaman, *Beilstein J. Org. Chem.*, 2010, **6**, 992–1001.
- 47 J. R. Lakowicz, Ed., *Principles of Fluorescence Spectroscopy*, Springer US, Boston, MA, 2006.
- 48 K. E. Linton, A. L. Fisher, C. Pearson, M. A. Fox, L.-O. Palsson, M. R. Bryce and M. C. Petty, *J. Mater. Chem.*, 2012, **22**, 11816–11825.
- 49 V. D. Gupta, V. S. Padalkar, K. R. Phatangare, V. S. Patil, P. G. Umape and N. Sekar, *Dye. Pigment.*, 2011, **88**, 378–384.
- 50 F. Würthner, T. E. Kaiser and C. R. Saha-Möller, *Angew. Chemie Int. Ed.*, 2011, **50**, 3376–3410.
- 51 K. R. Idzik, P. Ledwon, R. Beckert, S. Golba, J. Frydel and M. Lapkowski, *Electrochim. Acta*, 2010, **55**, 7419–7426.
- 52 P. Ledwon, M. Lapkowski, T. Licha, J. Frydel and K. R. Idzik, *Synth. Met.*, 2014, **191**, 74–82.
- 53 M. Lapkowski, J. Zak, K. Karon, B. Marciniec and W. Prukala, *Electrochim. Acta*, 2011, **56**, 4105–4111.
- 54 K. Karon and M. Lapkowski, *J. Solid State Electrochem.*, 2015, **19**, 2601–2610.
- 55 K. Laba, P. Data, P. Zassowski, K. Karon, M. Lapkowski, P. Wagner, D. L. Officer and G. G. Wallace, *Macromol. Rapid Commun.*, 2015, **36**, 1749–1755.
- 56 Y. Lin, H. Fan, Y. Li and X. Zhan, *Adv. Mater.*, 2012, **24**, 3087–3106.
- 57 E. T. Strom and G. A. Russell, *J. Am. Chem. Soc.*, 1965, **87**, 3326–3329.
- 58 S. Nowy, B. C. Krummacher, J. Frischeisen, N. A. Reinke and W. Brütting, *J. Appl. Phys.*, 2008, **104**.
- 59 T. Khanasa, N. Prachumrak, R. Rattanawan, S. Jungstittiwong, T. Keawin, T. Sudyoadsuk, T. Tuntulani and V. Promarak, *Chem. Commun.*, 2013, **49**, 3401–3403.
- 60 B. Qu, L. Feng, H. Yang, Z. Gao, C. Gao, Z. Chen, L. Xiao and Q. Gong, *Synth. Met.*, 2012, **162**, 1587–1593.
- 61 Z.-M. Tang, T. Lei, K.-J. Jiang, Y.-L. Song and J. Pei, *Chem. – An Asian J.*, 2010, **5**, 1911–1917.
- 62 D. Barpuzary, A. S. Patra, J. V. Vaghasiya, B. G. Solanki, S. S.

## ARTICLE

Journal Name

- Soni and M. Qureshi, *ACS Appl. Mater. & Interfaces*, 2014, **6**, 12629–12639.
- 63 A. D. Becke, *J. Chem. Phys.*, 1993, **98**, 5648–5652.
- 64 A. D. Becke, *J. Chem. Phys.*, 1993, **98**, 1372.
- 65 C. T. Lee, W. T. Yang and R. G. Parr, *Phys. Rev. B*, 1988, **37**, 785–789.
- 66 J. Tomasi, B. Mennucci and R. Cammi, *Chem. Rev.*, 2005, **105**, 2999–3093.
- 67 2009. Gaussian 09, Revision D.01, M. J. Frisch, G. W. Trucks, H. B. Schlegel, G. E. Scuseria, M. A. Robb, J. R. Cheeseman, G. Scalmani, V. Barone, B. Mennucci, G. A. Petersson, H. Nakatsuji, M. Caricato, X. Li, H. P. Hratchian, A. F. Izmaylov, J. Bloino, G. Zhe, .
- 68 A.-R. Allouche, *J. Comput. Chem.*, 2011, **32**, 174–82.
- 69 P. Stakhira, V. Cherpak, D. Volynyuk, F. Ivastchyshyn, Z. Hotra, V. Tataryn and G. Luka, *Thin Solid Films*, 2010, **518**, 7016–7018.
- 70 N. C. Greenham, R. H. Friend and D. D. C. Bradley, *Adv. Mater.*, 1994, **6**, 491–494.
- 71 Baldo, A. Marc, S. R. Forrest and M. E. Thompson, in *Organic Electroluminescence*, ed. Z. H. Kafafi, Taylor & Francis, New York, 2005.



64x32mm (300 x 300 DPI)